Factors Affecting the Damping Constant of a Spring System

Submitted for assessment in 12A_PHY1

James Bray

Christ Church Grammar School

2 September, 2025

Abstract

This investigation examines the effect of attached mass and spring configuration on the damping rate of a vertically oscillating mass-spring system. Displacement–time data was collected for varying load masses and spring arrangements to determine the decay constant γ and damped angular frequency ω'. Results showed that γ decreased with increasing mass, consistent with an inverse proportionality to m_{load}, while spring configuration indirectly produced small but measurable variations in damping, likely due to internal friction and alignment differences in the experimental setup. These findings provide empirical validation of theoretical damped harmonic motion models and highlight the strong interdependence of parameters in mechanical systems.

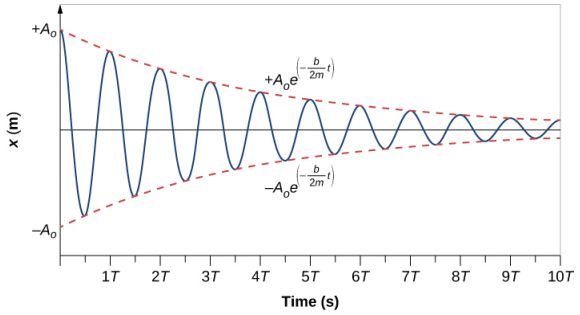

Figure 1: Displacement–time graph illustrating the characteristics of an underdamped harmonic oscillator.

1. Introduction

A vertical mass–spring system provides a simple model for studying oscillatory motion and energy dissipation in mechanical systems. An ideal mass–spring system undergoes simple harmonic motion with constant amplitude, but in real conditions mechanical energy is dissipated through a variety of means, causing oscillations to gradually decrease in amplitude. This phenomenon is known as damping, defined as "the loss of energy of an oscillating system by dissipation."

The degree of damping can be characterised by the decay constant γ which specifies the rate at which oscillations diminish, with larger values corresponding to faster energy loss. The value of this constant depends on both the properties of the oscillating mass and the restoring system.

1.1. Aim and Hypothesis

The aim of this investigation is to determine how spring configuration and attached mass influence the rate of damping, quantified by the exponential decay constant γ, in a vertically oscillating mass-spring system.

It is hypothesised that if the attached mass is increased, there will be a decrease in the decay constant γ proportional to ${m_{\text{load}}}^{-1}$, and if the spring system is configured in series, there will be no change in the decay constant.

The primary sources of damping are expected to be internal friction within the spring in conjunction with air resistance on the mass. For simplicity, it will be assumed that these factors can be modelled by a damping force which is linearly dependent on velocity, as with a standard viscous dampening model.

1.2. Variables

Independent Variables: The mass of the load attached to the end of the spring, and the configuration of the spring system.

Dependent Variable: The curve-fitting coefficients of the damped harmonic motion displacement-time graph.

Controlled Variables: The positioning of the retort stand and clamps, motion sensor alignment and sampling frequency, mass cross-sectional geometry, and ambient air conditions (temperature, pressure, humidity).

2. Theory

To model the motion mathematically, Newton's Second Law can be applied to the system for the applied, restoring, and damping forces. This results in a second-order differential equation that can be solved to find the displacement of the mass and the rate of amplitude decay, establishing the basis for determining k and b experimentally.

$$\begin{aligned}
\sum \vec{F} = m\vec{a} &= \vec{F}_{\text{restoring}} + \vec{F}_{\text{damping}} \\
m\vec{g} &= -k\vec{x} - b\vec{v} \\
0 &= k\vec{x} + b\frac{\mathrm{d}\vec{x}}{\mathrm{d}t} + m\frac{\mathrm{d}^2\vec{x}}{\mathrm{d}t^2} \\
0 &= k\vec{x} + b\frac{\mathrm{d}\vec{x}}{\mathrm{d}t} + m\frac{\mathrm{d}^2\vec{x}}{\mathrm{d}t^2} \\
0 &= \frac{k}{m}\vec{x} + \frac{b}{m}\frac{\mathrm{d}\vec{x}}{\mathrm{d}t} + \frac{\mathrm{d}^2\vec{x}}{\mathrm{d}t^2} \\
0 &= \frac{k}{m}e^{\lambda t} + \frac{b}{m}\frac{\mathrm{d}(e^{\lambda t})}{\mathrm{d}t} + \frac{\mathrm{d}^2(e^{\lambda t})}{\mathrm{d}t^2} \\
0 &= k + bu + m\lambda^2 \\
\lambda &= \frac{-b \pm \sqrt{b^2 - 4km}}{2m} \\
\lambda &= -\frac{b}{2m} \pm \frac{\sqrt{b^2 - 4km}}{2m}
\end{aligned}$$

It is assumed that the spring will be underdamped, meaning the damping is weak enough that the system oscillates around equilibrium before settling. Physically, this requires that $b^2 - 4km < 0$, so the displacement equation has complex roots and produces harmonic motion.

$$\implies \lambda = -\frac{b}{2m} \pm \frac{i\sqrt{4km - b^2}}{2m}$$

Given $\gamma = \frac{b}{2m}$ and $\omega' = \frac{\sqrt{4km-b^2}}{2m}$

$$\implies \lambda = -\gamma \pm i\omega'$$

The general solution for $\vec{x} = e^{\lambda t}$ is a linear combination of the solutions corresponding to each root λ, as required for a second-order differential equation.

$$\begin{aligned}
\vec{x} &= \alpha e^{(-\gamma + i\omega')t} + \beta e^{(-\gamma - i\omega')t} \\
&= e^{-\gamma t}\left[\alpha e^{i\omega' t} + \beta e^{-i\omega' t}\right] \\
&= e^{-\gamma t}\left[(\alpha + \beta)\cos(\omega' t) + i(\alpha - \beta)\sin(\omega' t)\right] \\
&= 2\sqrt{\alpha\beta}\, e^{-\gamma t}\cos(\omega' t + \phi)
\end{aligned}$$

Letting $A = 2\sqrt{\alpha\beta}$:

$$\therefore \vec{x} = Ae^{-\gamma t}\cos(\omega' t + \phi)$$

The oscillatory behaviour of a mass-spring system arises from the continual transformation between kinetic and potential energy, represented by the cosine term in the displacement equation. When the spring is displaced from its equilibrium position, potential energy is stored in the spring, and the speed of the mass decreases toward a minimum for that cycle. As the mass passes through equilibrium, this potential energy is converted almost entirely into kinetic energy, producing the maximum speed for the cycle.

However, this process is not perfectly efficient as the damping force removes energy from the system, predominantly as heat, which causes the amplitude of oscillations to decrease gradually over time. This decay is captured by the exponential term in the displacement equation. This process drives the sinusoidal and decaying components of motion, which are quantified by the damped angular frequency ω' and decay constant γ

The damped angular frequency ω' is dependent on both the spring constant k and the damping coefficient b, as evident in its formula $\omega' = \frac{\sqrt{4km-b^2}}{2m}$.

$$\begin{aligned}
\omega' &= \frac{\sqrt{4km - b^2}}{2m} \\
\omega'^2 &= \frac{k}{m} - \frac{b^2}{4m^2} \\
\omega'^2 &= \frac{k}{m} - \gamma^2 \qquad \text{with } \gamma = \frac{b}{2m} \\
\omega'^2 + \gamma^2 &= k\left(\frac{1}{m}\right)
\end{aligned}$$

As shown above, plotting $\omega'^2 + \gamma^2$ against m^{-1} should give a straight line with gradient k. The spring constant k represents the stiffness of the spring, and quantifies the relationship between the spring's restoring force and resulting displacement according to Hooke's law ($\vec{F}_{\text{restoring}} = -k\vec{x}$).

$$\begin{aligned}
\gamma &= \frac{b}{2m} \\
&= \frac{b}{2}\left(\frac{1}{m}\right)
\end{aligned}$$

Similarly, plotting the decay constant γ against m^{-1} should produce a straight line with gradient $b/2$, allowing determination of the damping coefficient b. This coefficient characterises the velocity-relative magnitude of the resistive force opposing motion, responsible for gradual reduction in oscillation amplitude.

3. Equipment and Method

3.1. Equipment

- 1 × LabQuest 2 and cables
- 1 × Vernier Motion Detector (±1 mm)
- 2 × Stiff springs
- 1 × Light spring
- 1 × Vernier Hanging Mass Set (250 g/50 g)
- 1 × Retort stand
- 1 × Bosshead clamp, spring hanger, and rod
- 1 × Scientific scale (±0.01 g)
- 1 × Computer with Logger Pro 3

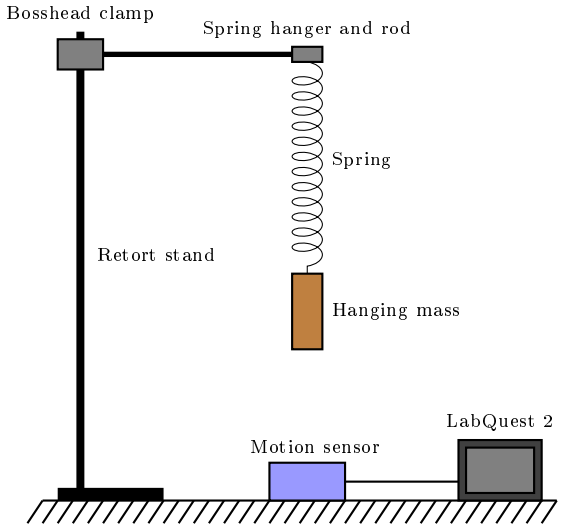

Figure 2: Experimental setup diagram for a vertical mass–spring system utilising a motion sensor.

3.2. Method

1. Set up equipment as depicted in Fig. 2, with the light spring hooked onto the spring hanger and base of the retort stand towards the mass.
2. Initialise the LabQuest 2 and Motion Detector and configure the mode to be displacement–time, sampling period to be 60 s, and sample rate to be 60 Hz.
3. Connect the LabQuest 2 wirelessly to a computer with Logger Pro running.
4. Measure and record the mass of the hanger from the Hanging Mass Set on a scientific scale.
5. Attach the mass to the end of the spring and release it in a controlled manner, ensuring there is no horizontal displacement of the system before starting the data recording from the computer.
6. Allow the 60 s data collection period to finish without disturbing the system before removing the mass from the spring system.
7. Apply a 'Damped Harmonic' curve fit in Logger Pro and record coefficients A, B, and C, and the R^2 value.
8. Place a 50 g mass from the Hanging Mass set onto the hanger and measure and record the new total mass.
9. Repeat steps 5 to 8 until at least 5 different masses have been trialled.
10. Replace the light spring with a stiff spring and repeat steps 5 to 9.
11. Replace the stiff spring with two stiff springs in series and repeat steps 5 to 9.

4. Results

Table 1: Regression parameters for the light spring.

m_{load} (kg)	γ (s^{-1})	ω' ($\text{rad}\,\text{s}^{-1}$)	R^2	${m_{\text{load}}}^{-1}$ (kg^{-1})	$\omega'^2+\gamma^2$ (s^{-2})
0.050 25	0.024 240	21.47	0.9990	19.90	461.0
0.100 14	0.019 520	15.43	0.8385	9.9860	238.1
0.150 44	0.015 780	12.53	0.9947	6.6472	157.0
0.200 11	0.012 860	10.89	0.9996	4.9973	118.6
0.250 19	0.012 236	9.75	0.9894	3.9970	95.1
0.300 12	0.011 830	8.92	0.9999	3.3320	79.5
0.349 91	0.011 380	8.28	0.9999	2.8579	68.6

Table 2: Regression parameters for the stiff spring.

m_{load} (kg)	γ (s^{-1})	ω' ($\text{rad}\,\text{s}^{-1}$)	R^2	${m_{\text{load}}}^{-1}$ (kg^{-1})	$\omega'^2+\gamma^2$ (s^{-2})
0.300 10	0.007 771	13.41	0.9971	3.3322	179.8
0.350 14	0.006 539	12.45	0.9955	2.8560	155.0
0.400 14	0.005 946	11.67	0.9993	2.4991	136.2
0.450 04	0.005 352	11.02	0.9993	2.2220	121.4
0.499 84	0.004 909	10.47	0.9995	2.0006	109.6

Table 3: Regression parameters for two stiff springs in series.

m_{load} (kg)	γ (s^{-1})	ω' ($\text{rad}\,\text{s}^{-1}$)	R^2	${m_{\text{load}}}^{-1}$ (kg^{-1})	$\omega'^2+\gamma^2$ (s^{-2})
0.300 10	0.004 957	9.581	0.9996	3.3322	91.80
0.350 14	0.004 321	8.907	0.9995	2.8560	79.33
0.400 14	0.003 469	8.363	0.9991	2.4991	69.94
0.450 04	0.003 112	7.907	0.9995	2.2220	62.52
0.499 84	0.002 791	7.517	0.9996	2.0006	56.51

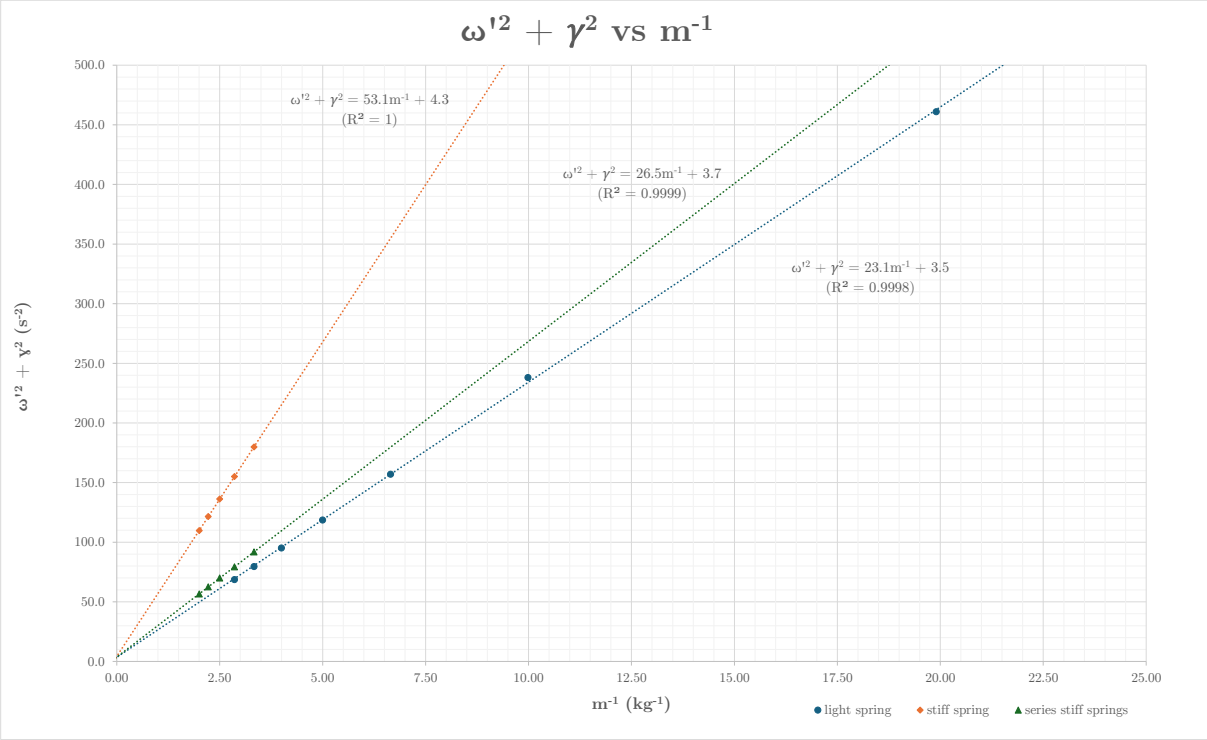

Graph 1: Relationship between $\omega'^2 + \gamma^2$ and ${m_{\text{load}}}^{-1}$ for different spring configurations, where the gradient represents the spring constant (k).

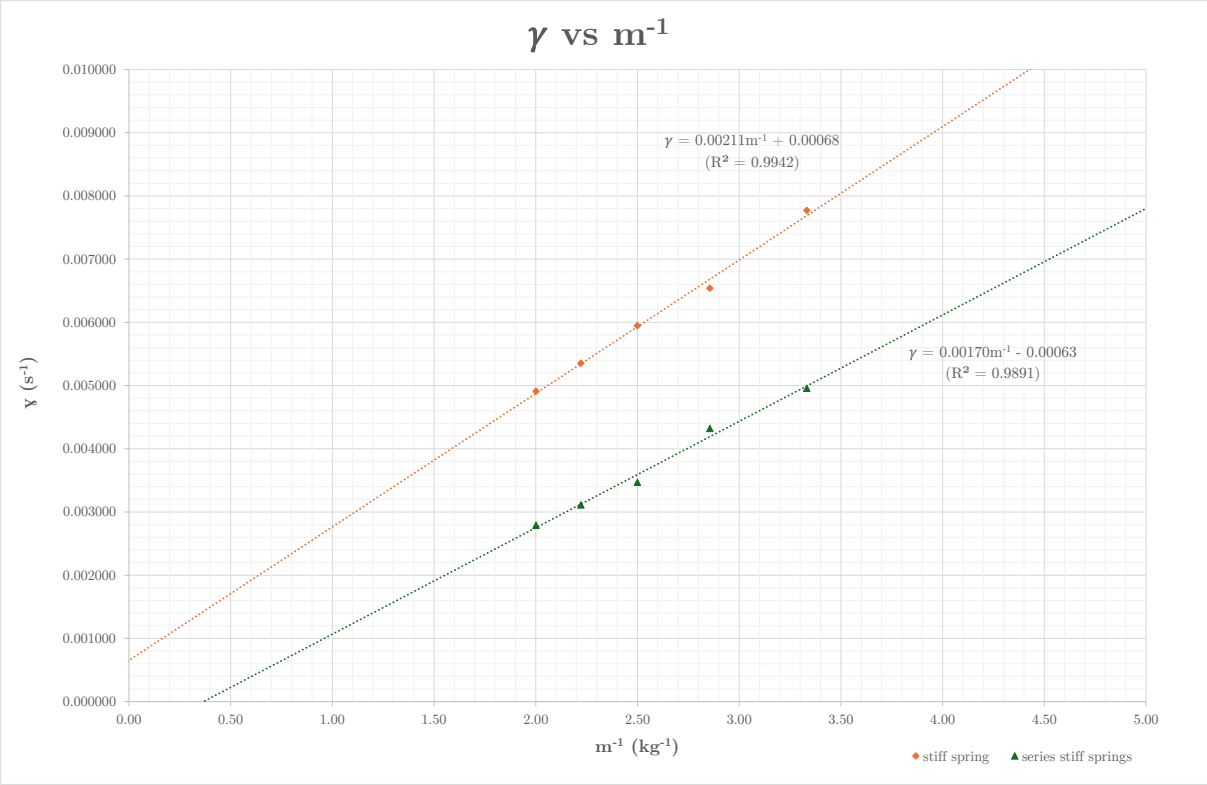

Graph 2: Relationship between γ and ${m_{\text{load}}}^{-1}$ for different spring configurations, where the gradient represents half the damping coefficient ($\frac{b}{2}$).

For **Graph 1**: $k =$ gradient.

$$\begin{aligned} k_{\text{light}} &= \frac{\Delta(\omega'^2 + \gamma^2)}{\Delta m_{\text{load}}^{-1}} \\ &= \frac{315.0 - 165.0}{13.50 - 7.00} \\ &= 23.1 \text{ kg s}^{-2} \text{ (3 s.f.)} \end{aligned}$$

$$\begin{aligned} k_{\text{single stiff}} &= \frac{\Delta(\omega'^2 + \gamma^2)}{\Delta m_{\text{load}}^{-1}} \\ &= \frac{375.0 - 30.0}{7.00 - 0.50} \\ &= 53.1 \text{ kg s}^{-2} \text{ (3 s.f.)} \end{aligned}$$

$$\begin{aligned} k_{\text{series series}} &= \frac{\Delta(\omega'^2 + \gamma^2)}{\Delta m_{\text{load}}^{-1}} \\ &= \frac{480.0 - 255.0}{18.00 - 9.50} \\ &= 26.5 \text{ kg s}^{-2} \text{ (3 s.f.)} \end{aligned}$$

For **Graph 2**: $b = 2 \times$ gradient.

$$\begin{aligned} b_{\text{single stiff}} &= 2 \times \frac{\Delta\gamma}{\Delta m_{\text{load}}^{-1}} \\ &= 2 \times \frac{(9.375 - 4.688) \times 10^{-3}}{4.12 - 1.90} \\ &= 4.22 \times 10^{-3} \text{ kg s}^{-1} \text{ (3 s.f.)} \end{aligned}$$

$$\begin{aligned} b_{\text{series stiff}} &= 2 \times \frac{\Delta(\omega'^2 + \gamma^2)}{\Delta m_{\text{load}}^{-1}} \\ &= 2 \times \frac{(6.875 - 1.250) \times 10^{-3}}{4.40 - 1.10} \\ &= 3.40 \times 10^{-3} \text{ kg s}^{-1} \text{ (3 s.f.)} \end{aligned}$$

Figure 3: Calculations of k and b values from graphs.

5. Analysis of Results

Analysis of the data in presented by **Graph 1** finds reasonably clear patterns emerging. By plotting the sum of the damped angular frequency squared and decay constant squared ($\omega'^2+\gamma^2$) against m_{load}^{-1}, a highly linear relationship between the variables can be observed. Forcing a linear line of best fit, the gradient is expected to yield the spring constant k. From the recorded data, the calculated spring constants are:

$$\begin{aligned} k_{\text{light}} &= 23.1 \text{kg s}^{-2} \\ k_{\text{single stiff}} &= 53.1 \text{kg s}^{-2} \\ k_{\text{series stiff}} &= 26.5 \text{kg s}^{-2} \end{aligned}$$

Given that the spring constant reflects the force required to stretch the spring a certain distance, it follows that the stiff spring has a higher k value than the light spring. Furthermore, the precision of the data can be testified by application of the general spring constant equation that states that the $k_{\text{equivalent}}$ of two identical springs in series is equal to $\frac{1}{2}k_{\text{single stiff}}$. From the measured $k_{\text{single stiff}}$, the theoretical equivalent series spring constant is $\frac{1}{2}(53.1) = 26.6$ (3 s.f.). This possesses a highly respectable percentage error of -0.376% between the calculated and empirical values, solidifying the relative precision between calculations.

Focusing on the tabulated data for the light spring, the curve fit for $m_{\text{load}} = 0.10014; \text{kg}$ exhibits an anomalously low R^2 value of 0.8385. During the data collection period, the spring system was observed to alternate between predominantly vertical oscillation and pendulum-like motion. This behaviour can be attributed to mode coupling, in which energy is transferred between distinct modes of motion, such that vertical oscillations couple to lateral or rotational motions. In this instance, near-resonance between the vertical spring mode and the pendulum mode allowed for periodic energy exchange between the modes, resulting in the observed switching between vertical and pendular motion. This violates the initial assumption of purely linear, one-dimensional motion, diminishing the quality of the exponential decay fit and indicating the presence of non-linear dynamics in low-mass, light spring configurations. It was not considered in the determination of the line of best fit in **Graph 1**.

Graph 2 depicts a slightly more ambiguous pattern. Unlike the clear proportionality observed in **Graph 1**, the relationship between γ and m_{load}^{-1} shows greater scatter, and the physical interpretation of the linear fit is less direct. Both the stiff spring and series stiff spring datasets still yield strong linear correlations ($R^2 = 0.9942$ and 0.9891 respectively), but the fitted lines have small but non-negligible intercepts, one positive and one negative. These offsets suggest influences outside the idealised damping model, such as frictional or measurement effects that contribute to a damping coefficient b independent of mass.

From the recorded data, the calculated damping coefficient values are:

$$b_{\text{single stiff}} = 4.22 \times 10^{-3} \text{kg s}^{-1}$$
$$b_{\text{series stiff}} = 3.40 \times 10^{-3} \text{kg s}^{-1}$$

To assess whether the difference in gradients and thus in the damping coefficient b between the single and series stiff spring datasets is statistically meaningful, 95% confidence intervals were calculated. As shown below, these intervals do not overlap, confirming that the difference in b is significant at the 5% level and supporting the interpretation that the spring configuration has a measurable effect on damping.

$$\bar{b}_{\text{single}} = 4.22 \times 10^{-3} \text{kg s}^{-1}, s.e.\left(b_{\text{single}}\right) = 0.00018$$

$$\begin{aligned} \text{C}_{95\%}\left(b_{\text{single}}\right) &= \bar{b}_{\text{single}} \pm (1.96 \times s.e.\left(b_{\text{single}}\right)) \\ &= 4.22 \times 10^{-3} \pm (1.96 \times 0.00018) \\ &= (4.22 \pm 0.353) \times 10^{-3} \\ &= (3.87,\ 4.57) \times 10^{-3} \text{ kg s}^{-1} \end{aligned}$$

$$\bar{b}_{\text{series}} = 3.40 \times 10^{-3} \text{kg s}^{-1}, s.e.\left(b_{\text{series}}\right) = 0.00020$$

$$\begin{aligned} \text{C}_{95\%}\left(b_{\text{series}}\right) &= \bar{b}_{\text{series}} \pm (1.96 \times s.e.\left(b_{\text{series}}\right)) \\ &= 3.40 \times 10^{-3} \pm (1.96 \times 0.00020) \\ &= (3.40 \pm 0.392) \times 10^{-3} \\ &= (3.01,\ 3.79) \times 10^{-3} \text{ kg s}^{-1} \end{aligned}$$

Figure 4: Calculations of 95% confidence intervals for the b values of the single and series configurations.

However, while the difference in damping coefficients is significant, it does not necessarily reflect a direct correlation to the physical configuration of the springs. It is more likely that the discrepancy arises primarily from the increase in total spring mass when an additional spring is added, uncovering a fundamental systematic issue within the method of calculation.

6. Evaluation

A significant systematic source of error in this investigation arises from neglecting the mass of the spring itself. The oscillating system's effective mass is not only from the attached load but includes a portion of the spring's mass, typically approximated as $m_{\text{equ}} = m_{\text{load}} + \frac{1}{3}m_{\text{spring}}$. Failure to account for this results in an overestimation of γ for a given m_{load}, particularly for lighter loads where the spring mass constitutes a larger fraction of the total oscillating mass. The impact can be quantified as shown below, demonstrating that neglecting the spring mass reduces the accuracy of the measured gradient in γ versus m_{load}^{-1}. To mitigate this, future analyses should explicitly include the spring's contribution to the effective mass in all calculations, ensuring that calculated parameters more accurately reflect the actual system values.

Let $m_{\text{equ}} = m_{\text{load}} + \frac{1}{3}m_{\text{spring}}$ and $\lambda = m_{\text{load}}^{-1}$

$$\begin{aligned} \gamma &= \frac{b}{2m_{\text{equ}}} \\ &= \frac{b}{2\left(m_{\text{load}} + \frac{1}{3}m_{\text{spring}}\right)} \\ &= \frac{b}{2\left(\frac{1}{\lambda} + \frac{1}{3}m_{\text{spring}}\right)} \\ &= \frac{b}{2}\frac{\lambda}{1 + \frac{1}{3}m_{\text{spring}}\lambda} \\ \therefore \frac{d\gamma}{d\lambda} &= \frac{b}{2}\frac{1}{\left(1 + \frac{1}{3}m_{\text{spring}}\lambda\right)^2} \end{aligned}$$

This form shows that the true relationship between γ and λ is not perfectly linear, with the denominator introducing a slight downwards concavity. A straight-line fit that assumes $\frac{1}{3}m_{\text{spring}} = 0$ therefore introduces a systematic error that always leads to an underestimation of b for a constant γ.

Graphically, this appears as a decreased gradient when plotting γ against m_{load}^{-1} and a slight nonlinearity, particularly at lower masses. Correcting for spring mass would both steepen the slope and improve linearity, yielding more accurate estimates of b from the decay constant.

Random errors also affected the investigation, particularly due to environmental and material factors. Uncontrolled air resistance introduces variability in the observed amplitude decay, reducing precision in the determination of γ across repeated trials. This can be minimised by conducting the experiment in a closed environment or vacuum chamber, thereby stabilising external forces acting on the oscillating mass. Additionally, plastic deformation of the springs over repeated oscillations alters their effective spring constants between trials, introducing both random and systematic deviations in measured γ and ω'. Using springs made from metals with low plasticity or replacing springs with near-perfect replicas between trials would reduce these effects, improving both the accuracy and reliability of results.

7. Conclusion

This investigation aimed to experimentally determine how spring configuration and attached mass influence the rate of damping, quantified by the exponential decay constant γ, in a vertically oscillating mass-spring system. The experiment involved the manipulation of the load mass attached to a spring system and measurement of displacement–over–time for the mass, leading to the determination of the coefficients γ and ω'.

My hypothesis was that if the attached mass m_{load} is increased, there will be a decrease in the decay constant γ proportional to ${m_{\text{load}}}^{-1}$, and if the spring system is configured in series, there will be no change in the decay constant. The results confirmed the inverse relationship between the decay constant and the load mass, with larger masses exhibiting slower exponential decay, consistent with the hypothesised proportionality.

To check the precision of the experiment, the spring constant of each spring configuration was determined and single vs series systems were compared producing a percentage error of -0.376%.

$$\begin{aligned} k_{\text{light}} &= 23.1\text{kg}\,\text{s}^{-2} \\ k_{\text{single stiff}} &= 53.1\text{kg}\,\text{s}^{-2} \\ k_{\text{series stiff}} &= 26.5\text{kg}\,\text{s}^{-2} \end{aligned}$$

For different spring configurations, the calculated values of b from the graph of γ and ${m_{\text{load}}}^{-1}$ showed small but statistically significant variation at the 5% level between series and single-spring setups, indicating that the spring arrangement had a tangible influence on decay constant under the conditions tested. This could be due to slight differences in friction or internal damping within the springs themselves, or small misalignments in the experimental setup that altered the effective damping. While there is a degree of uncertainty and a limited number of datapoints, the experiment stands as relatively sound, with sources of errors acknowledged and improvements suggested.

$$\begin{aligned} b_{\text{single stiff}} &= 4.22 \times 10^{-3}\text{kg}\,\text{s}^{-1} \\ b_{\text{series stiff}} &= 3.40 \times 10^{-3}\text{kg}\,\text{s}^{-1} \end{aligned}$$

Overall, the results confirm that the decay constant γ is inversely related to the effective mass and that spring configuration has an indirect yet measurable effect on damping, providing empirical support for the theoretical model.